Added Resistance by means of time-domain models in seakeeping

A. J. Hermans [1]

In many applications in seakeeping the added resistance plays an important role. It is observed that many of the existing methods underestimate the added resistance at low wave frequencies. This may be due to the way the potential is split up. It is shown that with the help of the steady wave potential obtained by RAPID a linearisation around the obtained steady free surface is possible and that the results obtained with a time-domain approach fit very well with the experimental results for an LNG-carrier obtained at MARIN. Also an asymptotic theory is presented that is able to predict the added resistance at low forward speed with rather simple means. In this case the problem is linearised with respect to the double body potential. Some results are shown for a circular cylinder.

Introduction

It is well known that to describe the motion of a ship sailing in waves strip-theory gives very good results for many practical hull forms. For this reason not much attention is paid to three dimensional solvers. In recent years computer programs are developed to compute the forces and motions of a ship sailing in waves by means of linear diffraction programs. These frequency-domain codes are in analogy with the programs developed for the zero speed case. This became possible since the one integral expression for the Green's function can be computed rather fast, so the main change in the zero-speed diffraction program is the use of a different subroutine for the Green's function. Also the extra terms in the pressure must be taken care of. In fact the method uses a linearisation around the unperturbed flow around the ship. This may be a good approximation for slender and thin ships. For this class of ships the strip-theory and its modifications give good results, as well. However, in the case of short waves these methods tend to underestimate the added-resistance severely. This becomes a problem if one tries to optimise a hull form if the average weather condition is taken into consideration. If the ship has a blunt hull-form the local steady flow influences the value of the added-resistance greatly. In this paper we present a time-domain method that is capable to solve different kinds of linearised formulations. As an input the program may use the unperturbed flow, double-body flow or the non-linear steady flow. In principle the method can be transformed into a non-linear solver. However, this has not been implemented yet. Experience with the raised panel code RAPID suggests that in the future a similar approach is possible for the unsteady part. The major part of this presentation is based on the PhD theses of Hoyte Raven [1] for the steady part and of Tim Bunnik [2] for the time-domain model.

The non-linear formulation

We consider a symmetrical, smoothly-shaped ship sailing with a constant velocity U in incoming waves that propagate in a direction which makes an angle θ with the forward direction of the ship. We choose a coordinate system fixed to the ship and moving with its mean velocity U. The frequency at which the incoming waves are encountered changes due to this forward speed, unless the ship sails in beam waves. The x-axis is along the direction of this current in the symmetry plane of the ship. The z-axis points upwards and the origin lies in the undisturbed free surface $z = 0$. The ship is free to rotate around or translate along any of its axes. The water depth h is supposed to be constant and, therefore, the bottom corresponds to the plane $z = -h$.

We assume that the flow is irrotational and incompressible, a velocity potential Φ exists, which gradient is the velocity of a fluid particle

$$\mathbf{u} = \nabla\Phi.$$

Inside the fluid domain this potential satisfies the equation of Laplace, which follows from the conservation of mass

$$\Delta\Phi = 0.$$

On the free surface two physical conditions hold. The first is the dynamic free-surface condition, stating that the pressure should equal the atmospheric pressure, which is true when we neglect surface tension. The pressure p inside the fluid follows from the equation of Bernoulli, which relates it to the velocity potential

$$-\frac{p-p_0}{\rho} = \frac{\partial\Phi}{\partial t} + \frac{1}{2}\nabla\Phi\cdot\nabla\Phi + gz - \frac{1}{2}U^2.$$

Imposing atmospheric pressure on the unknown free surface $z = \zeta$ gives the dynamic free-surface condition

$$\zeta = \frac{-1}{g}\left(\frac{\partial\Phi}{\partial t} + \frac{1}{2}\nabla\Phi\cdot\nabla\Phi - \frac{1}{2}U^2\right) \quad \text{on } z = \zeta. \tag{1}$$

The second is the kinematic condition, stating that a fluid particle cannot leave the free surface, which is mathematically described by

$$\frac{\partial\Phi}{\partial x}\frac{\partial\zeta}{\partial x} + \frac{\partial\Phi}{\partial y}\frac{\partial\zeta}{\partial y} + \frac{\partial\zeta}{\partial t} - \frac{\partial\Phi}{\partial z} = 0 \quad \text{on } z = \zeta.$$

If these two conditions are combined, the free-surface elevation ζ can be eliminated, resulting in a condition, on $z = \zeta(x,y,t)$, that contains the velocity potential only

$$g\frac{\partial\Phi}{\partial z} + \frac{\partial^2\Phi}{\partial t^2} + \nabla\Phi\cdot\nabla\frac{\partial\Phi}{\partial t} +$$

$$\left(\frac{\partial\Phi}{\partial x}\frac{\partial}{\partial x_\zeta} + \frac{\partial\Phi}{\partial y}\frac{\partial}{\partial y_\zeta}\right)\left(\frac{\partial\Phi}{\partial t} + \frac{1}{2}\nabla\Phi\cdot\nabla\Phi\right) = 0. \tag{2}$$

[1] *TU Delft, Faculty of Electrical Engineering, Mathematics and ComputerScience, Department of Applied Mathematical Analysis, Mekelweg 4, 2628 CDDelft, The Netherlands, e-mail a.j.hermans@ewi.tudelft.nl*

Care must be taken with the definition of the derivatives in this condition. The gradient, ∇, is defined as the vector with partial derivatives in x, y and z-direction. The partial derivatives $\frac{\partial}{\partial x_\zeta}$ and $\frac{\partial}{\partial y_\zeta}$, however, are here defined as operators working on a function that is defined at the free surface $z = \zeta$, so for $F = F(x, y, \zeta(x, y))$, these partial derivatives relate as follows to the partial derivatives $\frac{\partial}{\partial x}$ and $\frac{\partial}{\partial y}$

$$\frac{\partial F(x,y,\zeta(x,y))}{\partial x_\zeta} = \frac{\partial F}{\partial x} + \frac{\partial F}{\partial z}\frac{\partial \zeta}{\partial x}$$

and

$$\frac{\partial F(x,y,\zeta(x,y))}{\partial y_\zeta} = \frac{\partial F}{\partial y} + \frac{\partial F}{\partial z}\frac{\partial \zeta}{\partial y}.$$

So implicitly, the vertical partial derivative is hidden in these expressions. The partial derivatives $\frac{\partial}{\partial x_\zeta}$ and $\frac{\partial}{\partial y_\zeta}$ can be obtained by calculating the differences between points on the free surface, so we can use very simple difference schemes for a flat plane. We consider finite water depth, hence

$$\frac{\partial \Phi}{\partial n} = 0 \quad \text{at } z = -h.$$

The condition on the hull of the ship becomes

$$\frac{\partial \Phi}{\partial n} = \frac{\partial \boldsymbol{\alpha}}{\partial t} \cdot \mathbf{n} \quad \text{on } H(t), \tag{3}$$

where $\boldsymbol{\alpha}$ is the displacement and $H(t)$ the exact position of the hull in the mean ship-fixed coordinate system.

To obtain a unique solution, we have to impose a radiation condition. This condition states that waves generated by the ship should propagate away from the ship (in the steady case behind the ship).

Decomposition of the potential

It is very time consuming to solve the non-linear equations formulated in the previous section, especially when the ship has a forward speed and is sailing in waves. With the increase of computer power, non-linear calculations become moreand more promising. With the present state of computer technology, however, it is not yet possible to calculate the non-linear time-varying flow around a sailing ship within acceptable time limits yet. We therefore decided to split up the potential in a steady and an unsteady. For the time being the unsteady potential will be linearised. The appropriate small parameter is the wave steepness $\varepsilon = A/\lambda$, where A is the amplitude and λ the length of the time-dependent wave. The velocity potential is now decomposed into a steady, time-independent part Φ_s, and an unsteady, time-dependent part Φ_u,

$$\Phi(\mathbf{x}, t) = \Phi_s(\mathbf{x}) + \phi_u(\mathbf{x}, t). \tag{4}$$

For the steady potential $\Phi_s(\mathbf{x})$ several descriptions are used. for slender and/or thin ships it is common practice to replace this potential by the unperturbed steady potential Ux. The next step is that for slowly moving blunt bodies one replaces this by the double body potential or at finite forward speed by the solution of the non-linear problem. Before deriving the linearised equations for the unsteady potential we consider the steady potential in more detail.

The steady potential

We first consider the still water case, hence in front of the ship the free surface is unperturbed. The non-linear free surface conditions for the steady potential are

$$\frac{\partial \Phi_s}{\partial x}\frac{\partial \zeta_s}{\partial x} + \frac{\partial \Phi_s}{\partial y}\frac{\partial \zeta_s}{\partial y} - \frac{\partial \Phi_s}{\partial z} = 0 \quad \text{on } z = \zeta_s, \tag{5}$$

ζ_s is the steady free-surface elevation that satisfies

$$\zeta_s = -\frac{1}{2g}\left(\nabla\Phi_s \cdot \nabla\Phi_s - U^2\right). \tag{6}$$

On the hull, the steady flow satisfies the no-flux condition

$$\frac{\partial \Phi_s}{\partial n} = 0 \quad \text{on } H. \tag{7}$$

For a long time one has linearised these equations and solved the remaining linearised free surface condition. To compute this potential several methods are used. To compute the wave elevation along the hull the Dawson method is well known. It performs reasonably well for a variety of ship hulls. It is common practice to decompose the steady potential as follows

$$\Phi_s(\mathbf{x}) = \Phi_r(\mathbf{x}) + \phi(\mathbf{x}), \tag{8}$$

where $\Phi_r(\mathbf{x})$ equals the double body potential. This seems to make sense, however one must be a little bit more precise. The question is in what sense is this an asymptotic expansion. No mention is made about small parameters in this context. If one takes the slenderness parameter B/L or D/L where B is the beam and D is the draft of the ship and applies a straight forward perturbation technique it is consistent to replace the double body flow by the unperturbed flow Ux. It is well known that this leads to a non-uniform expansion near the bow and the stern of the ship, where a stagnation point is situated. Because of this phenomenon it is more convenient to look at the slow-ship linearisation first. This is done by several authors in the seventies and eighties. Well known is the work of Baba et al [3, 4], Newman [5], Eggers [6] and Brandsma [7] after the pioneering report of Ogilvie [8] in 1968. Brandsma ([9]) shows that a strickt expansion with respect to the Froude number, with the assumption that the potential function and its derivatives are of the same order of magnitude, the free surface condition as derived by Eggers is asymptotically consistent if applied at the double body free surface $z = \zeta_r$. If one introduced the new z coordinate $z' = z - \zeta_r$ and drops the primes in the coordinates, the free surface condition becomes

$$\begin{aligned}
&\phi_z + \frac{1}{g}\Big[\Phi_{rx}^2\phi_{xx} + 2\Phi_{rx}\Phi_{ry}\phi_{xy} + \Phi_{ry}^2\phi_{yy} + \\
&\left(3\Phi_{rx}\Phi_{rxx} + 2\Phi_{ry}\Phi_{rxy} + \Phi_{rx}\Phi_{rzz}\right)\phi_x + \\
&\left(3\Phi_{ry}\Phi_{ryy} + 2\Phi_{rx}\Phi_{rxy} + \Phi_{ry}\Phi_{rxx}\right)\phi_y\Big] = D(x,y) \;\text{ at }\; z = 0,
\end{aligned} \tag{9}$$

where $D(x,y)$ is determined by the double body potential. We have

$$D(x,y) = \frac{\partial}{\partial x}\left[\zeta_r(x,y)\Phi_{rx}(x,y,0)\right] + \frac{\partial}{\partial y}\left[\zeta_r(x,y)\Phi_{ry}(x,y,0)\right] \tag{10}$$

and

$$\zeta_r = \frac{1}{2g}\left[U^2 - \Phi_{rx}^2(x,y,0) - \Phi_{ry}^2(x,y,0)\right]. \tag{11}$$

The transformation generates some extra terms in the potential equation that may be neglected as is shown by Brandsma [9]. The condition advocated by Dawson [10],

$$\left(\Phi_{rl}^2\phi_l\right)_l + g\phi_z = 2\Phi_{rl}^2\Phi_{rll}, \tag{12}$$

where l is a curvilinear coordinate along the streamlines of the double body flow on the undisturbed free surface, is a simplified version of the condition given here. It is shown by Brandsma [7] that the boundary value problem as described here is suitable for a direct application of the short wave theory, ray method, as developed in short waves acoustics for instance. For the determination of the excitation coefficients, initial conditions for the phase function along the rays generated at the sharp bow and stern, use is made of the asymptotic evaluation of the local free surface source distribution. This distribution can also be found in the work of Baba. The asymptotic results are derived for a limited class of bow shapes, hence its application is limited. In principle the method can be extended to more general hull shapes, however, more effort has been put in the numerical evaluation of complete nonlinear methods. Raven [1] gives an overview of the advantages and disadvantages of the use of the different linearised versions of the free surface conditions. At first he developed a numerical code consisting of a source distribution along the ship hull and the free surface. Starting with the Dawson condition it seemed that good results could be obtained. It turned out that this was true in a limited number of cases. Although the asymptotic results obtained by Brandsma [7] showed that certain features could be represented very well by (9), implementation in the numerical code did not show sufficient improvement. Especially the computation of the wave resistance gave negative values at low speed, for both the free surface condition (9) and the ones of Dawson [10] and Eggers [6]. This was not observed in the asympotic theory ([7]), because there the wave resistance was computed by means of the far field wave pattern.

Finally Raven [1] decided to solve the nonlinear problem. One way to do so is to write the velocity potential in the fluid domain as a source distribution as follows.

$$\Phi_s(\mathbf{x}) = \Phi_\infty(\mathbf{x}) + \int\int_{\partial D} \sigma(\boldsymbol{\xi}) G(\boldsymbol{\xi};\mathbf{x})\, \mathrm{d}S_\xi, \tag{13}$$

where for deep water the Green's function is chosen as

$$G(\boldsymbol{\xi};\mathbf{x}) = -\frac{1}{4\pi r} \qquad r = |\mathbf{x} - \boldsymbol{\xi}|.$$

The integration may be chosen along the ship hull and the actual free surface. However, it turns out to be very convenient to replace this distribution along the unknown free surface by a distribution along a surface above the free surface. This raised panel method has been applied by several authors and it turns out to be an efficient method. An iteration scheme is started where in each step the free surface is updated by means of the dynamic free surface condition. The collocation points are chosen at the body and the updated free surface. To avoid oscillations in the source strength the collocation points areshifted forward.

To obtain a solution that reproduces the physical state properly one must compare the dispersion relation of the numerical scheme with the one exact one. Based on the investgations of Sclavounos and Nakos [11], Raven [1] gives a thorough accuracy analysis for the 2-d case. The raised panels and the position of the collocation points generate an error in the numerical dispersion relation. Raven [1, 12] uses the notation of Sclavounos et al [11]

$$s := \frac{k\Delta x}{2\pi} \qquad F_{n\Delta} := \frac{U_\infty}{\sqrt{g\Delta x}}. \tag{14}$$

The continuous *dispersion* expression or the denominator in the expression for the Fourier transform of for instance the source function becomes

$$\widetilde{\mathcal{W}_\nu} = k_0 - k = k_0(1 - 2\pi F n_\Delta^2 s). \tag{15}$$

The dispersion relation for the discrete operator becomes

$$\widehat{\mathcal{W}_\nu} = k_0(1 - 2\pi F n_\Delta^2 Lh(s)). \tag{16}$$

In the unsteady part we will use the notation

$$k_d = k_c(1 + C_r + \mathrm{i}C_i) \tag{17}$$

In the Figures 1 and 2 the parameter α expresses the distance of the

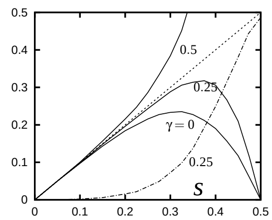

Figure 1: $\Re Lh(s)$ for $\alpha = 0.5$ and $\gamma = 0.5,\ 0.25,\ 0$ and $\Im Lh(s)$ for $\gamma = 0.25$.

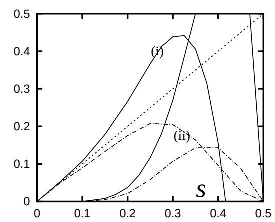

Figure 2: $\Re$ and $\Im Lh(s)$ (i) for $\alpha = 1,\ \gamma = 0.25$ and Dawson (ii).

raised panels with respect to the actual free surface $y_{fs} = \alpha\Delta x$ and γ expresses the upstream shift, $\gamma\Delta x$, of the collocation points. Figure 1 shows the numerical errors caused by the discretisation of the source distribution only. The full lines indicate the real part of $Lh(s)$, which ought to correspond with the diagonal line $Lh(s) = s$. The horizontal deviation from the diagonal indicates the numerical dispersion, which appears to depend on the collocation point shift γ but is almost zero for lower s (dense panellings). The dotted line is $\Im\ Lh(s)$ and indicates a numerical damping. The collocation point shift is selected such as to give large damping for large s values ($s > 0.2$, less than 5 panels per wavelength) and remove any susceptibility for oscillations. Figure 2 shows a similar result, but including the errors due to the use of a difference scheme in the FSBC. The full line is the raised-panel method, which has third-order dispersion and a large damping at $s = 0.5$ (two panels per wavelength). The dotted line is the usual method with panels on the water surface, which leads to first-order numerical dispersion and zero damping at $s = 0.5$ (causing point-to-point oscillations). Based on such considerations Raven [12] designed and implemented, for useful values of s, a special low-damping scheme.

The computer code RAPID is used extensively for many different practical hull forms. Since 1994 the code is being applied at MARIN in practical ship design projects, now at a rate of several hundreds of calculations per year. It has been installed at several shipyards and universities.

The unsteady potential

We first decompose the free surface elevation in a steady and an unsteady component as well. The total free surface elevation is written as

$$\zeta_t(x,y,t) = \zeta_s(x,y) + \zeta_u(x,y,t) \tag{18}$$

where the steady level ζ_s is given in (6). If we retain linear terms with respect to the unsteady potential the unsteady contribution becomes

$$\zeta_u = -\frac{1}{g}\left(\frac{\partial\phi_u}{\partial t} + \nabla\Phi_s \cdot \nabla\phi_u\right) \Big/ \left(1 + \frac{1}{2g}\frac{\partial}{\partial z}\left(\nabla\Phi_s \cdot \nabla\Phi_s\right)\right) \tag{19}$$

on $z = \zeta_s$. If we now retain the linear terms with respect to $\phi_u(\vec{x},t)$ in the expression for the dynamic and kinematic free surface condition and eliminate the free surface elevation we obtain the result derived by Newman [13] in 1978 and used by Bertram [14] in 1996. The final expression is transferred to a condition along the steady free surface $z = \zeta_s$, we obtain

$$\begin{aligned} &\frac{\partial^2\phi_u}{\partial t^2} + 2\nabla\Phi_s \cdot \nabla\frac{\partial\phi_u}{\partial t} + \nabla\Phi_s \cdot \nabla\left(\nabla\Phi_s \cdot \nabla\phi_u\right) + \\ &\frac{1}{2}\left(\frac{\partial\phi_u}{\partial x}\frac{\partial}{\partial x_{\zeta_s}} + \frac{\partial\phi_u}{\partial y}\frac{\partial}{\partial y_{\zeta_s}}\right)\|\nabla\Phi_s\|^2 + g\frac{\partial\phi_u}{\partial z} + \\ &\zeta_u\frac{\partial}{\partial z}\left(\frac{1}{2}\left(\frac{\partial\Phi_s}{\partial x}\frac{\partial}{\partial x_{\zeta_s}} + \frac{\partial\Phi_s}{\partial y}\frac{\partial}{\partial y_{\zeta_s}}\right)\|\nabla\Phi_s\|^2 + g\frac{\partial\Phi_s}{\partial z}\right) = 0. \end{aligned} \tag{20}$$

Far away from the ship, where the steady flow is uniform, so $\Phi_s = Ux$, this condition reduces to the Kelvin condition

$$\frac{\partial^2\phi_u}{\partial t^2} + 2U\frac{\partial^2\phi_u}{\partial x\partial t} + U^2\frac{\partial^2\phi_u}{\partial x^2} + g\frac{\partial\phi_u}{\partial z} = 0 \quad \text{on } z = 0. \tag{21}$$

When we compare these two linear free-surface conditions, it can be seen that the first contains two extra terms compared to the second one. The first extra term is a term with the products of unsteady velocities and partial derivatives of the squared velocity along the steady free surface. The second extra term is a transfer term which is included because the free-surface condition is imposed on the steady free surface instead of on the actual free surface. Both terms contain first and/or second derivatives of the steady velocity. If we want to use condition (20) we must first make sure that these derivatives can be calculated accurately.

The boundary condition on the hull (3) is non-linear in the sense that it is imposed on a moving boundary $H(t)$, which position is part of the solution and not known in advance. Timman and Newman [15] showed that if the displacement relative to the mean position of the ship is small, the boundary condition can be linearized about the mean position by using a Taylor expansion. To guarantee a small displacement, the amplitude of the incoming waves must be small, and the frequency of the incoming wave may not be near the eigen-frequency of the ship. This is because a small force near the eigen-frequency can still lead to large ship motions. The Taylor expansion results in the following condition

$$\frac{\partial\phi_u}{\partial n} = \frac{\partial\boldsymbol{\alpha}}{\partial t}\cdot\mathbf{n} + \left(\left(\nabla\Phi_s\cdot\nabla\right)\boldsymbol{\alpha} - \left(\boldsymbol{\alpha}\cdot\nabla\right)\nabla\Phi_s\right)\cdot\mathbf{n} \tag{22}$$

where $\boldsymbol{\alpha}$ is the total first-order displacement vector, consisting of a translation $\mathbf{X}$ and a rotation $\boldsymbol{\Omega}$ relative to the centre of gravity of the ship $\mathbf{x}_g$, so

$$\boldsymbol{\alpha} = \mathbf{X} + \boldsymbol{\Omega}\times\left(\mathbf{x}-\mathbf{x}_g\right). \tag{23}$$

As can be seen, the hull boundary condition not only contains steady velocitieson the hull, but also their derivatives. These derivatives must be examined carefully, because it can be hard to determine them accurately. Especially near stagnation points like for example at a blunt bow, it can be impossible to do so.

The radiation condition can be fulfilled in several ways. Depending on the forward speed one may choose differently. First we notice that in the far field the steady potential can be replaced the unperturbed flow. Hence, the free surface condition (21) is applicable in the outer region. In the case of low speed Sierevogel[16] chooses a variation of the Dirichlet to Neuman (DtN) method. This method for time discretised problems is described in Givoli [17]. What the method does is that for the time discretised problem the far field solution is written in the form of a series expansion or a Green's representation. In this way a relation between the value of the potential and it normal derivative at the boundary of the computational domain is obtained. For many problems the choice of eigenfunctions works well, however in the case of water waves a severe convergence problem arises due to the form of the eigenfunctions. On the other hand application of the Green theorem is very efficient due to the special form of the appropriate Green's function. In the case of finite and high speed an appropriate choice to force outgoing diffracted waves is to apply a damping zone. A way to do this is to add an artificial damping term to the free surface condition. For instance

$$\nu(x,y)\left(\frac{\partial\phi_u}{\partial t} + \nabla\Phi_s\cdot\nabla\phi_u\right)$$

is a good choice. The artificial damping $\nu(x,y)$ is chosen to be continuous and such that it is zero in the domain of interest and increasing to a finite value in the damping zone. In this case the waves are diffracted and radiated behind the ship and if some reflection occurs the computational domain is chosen such that the waves reflected at the outer boundary do not reach the ship.

The first order forces acting on the ship can be expressed in the following way

$$\begin{aligned} \mathbf{F}_u^{(1)} = &\iint_{\overline{H}}\left(p_{H_u}^{(1)}\overline{\mathbf{n}} + p_{H_s}\mathbf{n}_u^{(1)}\right)\,\mathrm{d}S = \\ -\rho &\iint_{\overline{H}}\left(\frac{\partial\phi_u}{\partial t} + \nabla\Phi_s\cdot\nabla\phi_u\right)\overline{\mathbf{n}}\,\mathrm{d}S + \\ &\iint_{\overline{H}}\left(p_s\boldsymbol{\Omega}\times\overline{\mathbf{n}} + \left(\mathbf{X}^{(1)} + \boldsymbol{\Omega}\times\left(\overline{\mathbf{x}}-\mathbf{x}_g\right)\right)\cdot\nabla p_s\overline{\mathbf{n}}\right)\,\mathrm{d}S. \end{aligned} \tag{24}$$

The superscript$^{(1)}$ indicates the first order dynamic pressure and normal vector. The overbar indicates the mean position of the hull and its coordinate system. In the thesis of Bunnik the choice has been made to follow the same method of potential splitting as is done in the frequency domain commonly. In principle one can compute the excitation and reaction forces at once each time step, while solving the equations of motion at the same time. This approach is not followed here, to make a comparison with frequency results easier. One likes to compare added mass and wave damping easily.

We are also interested in a higher order effect, namely the wave resistance. This second order force is the time averaged second order force acting on a ship sailing in monochromatic waves. So instead of considering general time dependent incident sea states one looks at the frequency components separately. The added resistance, constant for each frequency, can be written as

$$\begin{aligned} \left\langle\mathbf{F}^{(2)}\right\rangle = &\left\langle -\frac{1}{2}\rho\iint_{\overline{H}}\nabla\phi_u\cdot\nabla\phi_u\overline{\mathbf{n}}\,\mathrm{d}S + \right. \\ &\iint_{\overline{H}}\left(\boldsymbol{\Omega}\times\left(\boldsymbol{\Omega}\times\left(\overline{\mathbf{x}}-\mathbf{x}_g\right)\right)\right)\cdot\nabla p_s\overline{\mathbf{n}}\,\mathrm{d}S + \boldsymbol{\Omega}\times\left(M\frac{\partial^2\mathbf{X}}{\partial t^2}\right) \\ -\rho &\iint_{\overline{H}}\left(\boldsymbol{\alpha}\cdot\nabla\right)\left(\nabla\Phi_s\cdot\nabla\phi_u + \frac{\partial\phi_u}{\partial t}\right)\overline{\mathbf{n}}\,\mathrm{d}S + \end{aligned} \tag{25}$$

$$\rho g \int_{wl} \zeta_u (\zeta_u - \alpha_3) \overline{\mathbf{n}} \, dl + \frac{1}{2} \int_{wl} \frac{\partial p_s}{\partial z}\bigg|_{z=\zeta_s} \left({\zeta_u}^2 - {\alpha_3}^2 \right) \overline{\mathbf{n}} \, dl \bigg\rangle.$$

We omitted the second order quantities in these expressions because only quadratic terms of first order quantities contribute to the avaraged second order forces. If we are interested in slowly varying second order forces we must take care of the second order potential as well.

Asymptotic and numerical formulation

To get some insight in the significance of a proper description of the free surface condition in the numerical scheme we consider an asymptotic formulation first. For short waves Hermans [18] applied an asymptotic ray method to determine the influence of the local flow field near a stagnation point. It is shown that at low speed the distortion of the wave pattern due to the local double body potential flow influences the added resistance greatly. Kalske [19] extended this approach to more general hull forms.

Asymptotic formulation

We first describe the asymptotic method as described by Hermans [18] and Kalske [19] . In this approach the Froude number, defined with respect to the length of the ship, $Fn = U/\sqrt{gL}$ is assumed to be small. In this case the steady potential $\Phi_s(\vec{x})$ can be replaced by the double body potential $\Phi_r(\vec{x})$. It is shown by Sakamoto and Baba [20] that after the coordinate transformation

$$x' = x, \quad y' = y, \quad z' = z - \zeta_r(x,y,)$$

the boundary condition for the unsteady wave potential $\phi(\mathbf{x},t)$, after omitting primes becomes,

$$\frac{1}{g}\left[\frac{\partial}{\partial t} + u\frac{\partial}{\partial x} + v\frac{\partial}{\partial y}\right]^2 \phi + \frac{\partial}{\partial z}\phi = 0 \quad \text{on } z = 0, \tag{26}$$

where ζ_r is the free surface elevation due to ϕ_r and the velocity $\mathbf{u} = \nabla\phi_r$ is calculated at the undisturbed free surface. The terms in this expression must be of the same order of magnitude. This is the case if the frequency of the waves is large, while the dimensionless parameter $\tau = \omega U/g$ remains finite. It has been shown in [20] that the neglected terms in the free surface condition are small in this situation.

The potential function $\phi(\mathbf{x},t)$ obeys the Laplace equation

$$\Delta\phi = 0 \quad \text{in the fluid} \tag{27}$$

and on the ship's hull we have $\frac{\partial\phi}{\partial n} = 0$. At infinity the incoming wave field consists of a plane wave

$$\phi_{\text{inc}} = \, e^{ik_0(x\cos\theta + y\sin\theta) + k_0 z - i\omega t}, \tag{28}$$

where $k_0 = \omega_0^2/g$ for deep water and $\omega = \omega_0 + k_0 U\cos\theta$ is the relative frequency. We consider short waves with respect to the ship length L, i.e. $k_0 L = \omega_0^2 L/g \ll 0$. However it is more convenient to choose $k = \omega^2/g$ as large parameter.

We introduce the well known ray expansion

$$\phi(\mathbf{x},t;k) = a(\mathbf{x},k)\, e^{ikS(\mathbf{x}) - i\omega t}, \tag{29}$$

where $S(\mathbf{x})$ is the phase function and $a(\mathbf{x},k)$ the amplitude function. The latter is written as a regular series expansion with respect to inverse powers of ik,

$$a(\mathbf{x},k) = \sum_{j=0}^{N} \frac{a_j(\mathbf{x})}{(ik)^j} + o((ik)^{-N}). \tag{30}$$

We restrict ourselves to the determination of $S(\mathbf{x})$ and $a_0(\mathbf{x})$.

Insertion of (29) into the Laplace equation (27) gives

$$-k^2 a\nabla_3 S\cdot\nabla_3 S + ik(2\nabla_3 a\cdot\nabla_3 S + a\Delta_3 S) + O(1) = 0. \tag{31}$$

The subscript 3 is used to indicate the three-dimensional ∇ and Δ operator. If no subscript is used the operator acting on S or a_0 is two-dimensional in the horizontal plane. Comparing orders of magnitude in (31) leads to a set of equations for S and a_0 to be satisfied in the fluid region:

$$\left.\begin{array}{ll} O(k^2): & \nabla_3 S\cdot\nabla_3 S = 0 \\ O(k^1): & 2\nabla_3 a_0\cdot\nabla_3 S + a_0\Delta_3 S = 0 \end{array}\right\} \text{ in the fluid.} \tag{32}$$

Next we insert (29) into the free-surface condition (26) and obtain

$$-k^2\{(1-\mathbf{u}\cdot\nabla S)^2 - iS_z\}a - ik\{2\mathbf{u}\cdot\nabla a - 2(\mathbf{u}\cdot\nabla S)(\mathbf{u}\cdot\nabla a) -$$

$$\mathbf{u}\cdot\nabla(\mathbf{u}\cdot\nabla S)a + ia_z\} + O(1) = 0. \tag{33}$$

Comparing orders of magnitude in (33) yields

$$\left.\begin{array}{ll} O(k^2): & iS_z = (1-\mathbf{u}\cdot\nabla S)^2 \\ O(k^1): & a_{0z} = i\{2\mathbf{u}\cdot\nabla a_0 - 2(\mathbf{u}\cdot\nabla S)(\mathbf{u}\cdot\nabla a_0) \\ & \qquad -\mathbf{u}\cdot\nabla(\mathbf{u}\cdot\nabla S)a_0\} \end{array}\right\} \text{ at } z=0. \tag{34}$$

The equations for the phase function at the free surface is obtained by elimination of S_z. Equations (32) and (34) yield the eikonal equation

$$(1-\mathbf{u}\cdot\nabla S)^4 - \nabla S\cdot\nabla S = 0, \tag{35}$$

and the transport equation

$$\{2\nabla S + 4(1-\mathbf{u}\cdot\nabla S)^3\mathbf{u}\}\cdot\nabla a_0 + a_0 MS = 0, \tag{36}$$

where $MS = \Delta_3 S - 2\mathbf{u}\cdot\nabla(\mathbf{u}\cdot\nabla S)(1-\mathbf{u}\nabla S)^2$. In order to solve the eikonal equation (35) we introduce the notation $\mathbf{p} = (p,q) := (S_x, S_y)$ and write (35) in the standard form $F(x,y,S,p,q) = 0$ and apply the method of characteristics. The equations for the characteristics are the Charpit-Lagrange equations:

$$\begin{aligned} \frac{dx}{d\sigma} &= F_p = -4(1-\mathbf{u}\cdot\mathbf{p})^3 u - 2p, \\ \frac{dy}{d\sigma} &= F_p = -4(1-\mathbf{u}\cdot\mathbf{p})^3 v - 2q, \\ \frac{dp}{d\sigma} &= -(F_x + pF_S) = 4(1-\mathbf{u}\cdot\mathbf{p})^3(\mathbf{u}_x\cdot\mathbf{p}), \\ \frac{dq}{d\sigma} &= -(F_y + qF_S) = 4(1-\mathbf{u}\cdot\mathbf{p})^3(\mathbf{u}_y\cdot\mathbf{p}). \end{aligned} \tag{37}$$

The solutions of these equations (37) are called *rays* as in geometrical optics. The phase function is obtained by solving the equation

$$\frac{dS}{d\sigma} = pF_p + qF_q = -4(1-\mathbf{u}\cdot\mathbf{p})^3 + 2\mathbf{p}\cdot\mathbf{p}. \tag{38}$$

One must realise that the rays are not perpendicular to the wave fronts S =constant. The transport equation along the rays becomes

$$\frac{da_0}{d\sigma} = a_0 MS. \tag{39}$$

This operator MS has the final form

$$
\begin{aligned}
MS &= S_{xx}\left\{1-2|\nabla S|u^2-\frac{S_x^2}{S_x^2+S_y^2}\right\}+ \\
&\quad S_{xy}\left\{-4|\nabla S|u^2-2\frac{S_xS_y}{S_x^2+S_y^2}\right\}+ \qquad (40)\\
&\quad S_{yy}\left\{1-2|\nabla S|u^2-\frac{S_x^2}{S_x^2+S_y^2}\right\}-2|\nabla S|\nabla(\mathbf{u}\cdot\mathbf{u})\cdot\nabla S.
\end{aligned}
$$

Before we can solve the characteristic equations together with the phase and amplitude function the second derivatives in MS must be determined. Hermans [18] used numerical differentiation to do so while Kalske [19] used the ordinary differential equations for those terms,

$$
\begin{aligned}
\frac{\mathrm{d}p_x}{\mathrm{d}\sigma} &= 12(1-\mathbf{u}\cdot\mathbf{p})^2(\mathbf{u}\cdot\mathbf{p})_x^2-2\mathbf{p}_x\cdot\mathbf{p}_x- \\
&\qquad 4(1-\mathbf{u}\cdot\mathbf{p})^3(\mathbf{u}_{xx}\cdot\mathbf{p}+2\mathbf{u}_x\cdot\mathbf{p}_x), \\
\frac{\mathrm{d}p_y}{\mathrm{d}\sigma} &= 12(1-\mathbf{u}\cdot\mathbf{p})^2(\mathbf{u}\cdot\mathbf{p})_x(\mathbf{u}\cdot\mathbf{p})_y-2\mathbf{p}_x\cdot\mathbf{p}_y- \\
&\qquad 4(1-\mathbf{u}\cdot\mathbf{p})^3(\mathbf{u}_{xy}\cdot\mathbf{p}+\mathbf{u}_x\cdot\mathbf{p}_y+\mathbf{u}_y\cdot\mathbf{p}_x), \qquad (41)\\
\frac{\mathrm{d}q_y}{\mathrm{d}\sigma} &= 12(1-\mathbf{u}\cdot\mathbf{p})^2(\mathbf{u}\cdot\mathbf{p})_y^2-2\mathbf{p}_y\cdot\mathbf{p}_y- \\
&\qquad 4(1-\mathbf{u}\cdot\mathbf{p})^3(\mathbf{u}_{yy}\cdot\mathbf{p}+2\mathbf{u}_y\cdot\mathbf{p}_y),
\end{aligned}
$$

The characteristic equations together with the equations along these characteristics can be solved. We give initial conditions for the incident field at a distance from the object where the ray pattern is not disturbed by the double body potential. These ordinary differential equation are solved by RK4. At the object we take care of the proper reflection laws generated by the Neumann boundary condition (no flux).

The mean resistance $\mathbf{F}_{aw}$ is defined as the time-averaged force acting on the hull, due to waves. The force in the $x-$direction is the added resistance. In general we have

$$
\mathbf{F}_{aw} = -\overline{\int_{z=-\infty}^{\zeta}\int_{\mathrm{WL}} p\mathbf{n}\,\mathrm{d}l\,\mathrm{d}z}. \qquad (42)
$$

In the asymptotic case this leads to the expression

$$
\begin{aligned}
\mathbf{F}_{aw} &= \qquad (43)\\
&-\frac{1}{4}\int_{\mathrm{WL}}\left\{\left(\nabla S^{(i)}\cdot\nabla S^{(i)}\right)^{\frac{1}{4}}a_0^{(i)}+\left(\nabla S^{(r)}\cdot\nabla S^{(r)}\right)^{\frac{1}{4}}a_0^{(r)}\right\}^2\mathbf{n}\,\mathrm{d}l \\
&+\frac{1}{4}\int_{\mathrm{WL}}\left\{a_0^{(i)^2}\left|\nabla S^{(i)}\right|+a_0^{(r)^2}\left|\nabla S^{(r)}\right|+\right. \\
&\left. 2a_0^{(i)}a_0^{(r)}\frac{\nabla S^{(i)}\cdot\nabla S^{(r)}+\left|\nabla S^{(i)}\right|\left|\nabla S^{(r)}\right|}{\left|\nabla S^{(i)}\right|+\left|\nabla S^{(r)}\right|}\right\}\mathbf{n}\,\mathrm{d}l.
\end{aligned}
$$

The superscripts for the amplitude and the face indicate incoming and reflected waves. In the Figures 3 and 4 we give results of the ray pattern for a circular cylinder in deep water for $\theta = 0^\circ$ and $\tau = 0.25$ and $\tau = 0.5$. In Figure 5 the values of the mean forces are given for a circular cylinder and a sphere. In the Figure 4 we see that in front of the blunt bow the reflected rays form a caustic. The amplitudes near this line becomes infinite. In principal one can derive a uniformly valid asymptotic theory with finite amplitude near this line, see Hermans [22]. It has been shown that the waves become shorter and the amplitude larger near the caustic. The result of this is that the wave break in front of the blunt bow, even in the case of low incident waves. This is observed in practice as well.

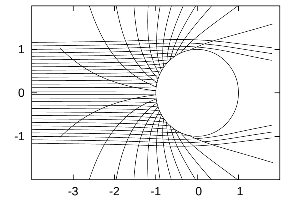

Figure 3: Ray pattern for a cylinder with $\tau = 0.25$

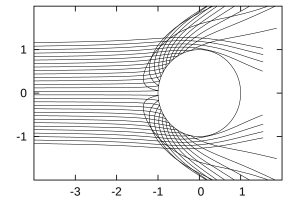

Figure 4: Ray pattern for a cylinder with $\tau = 0.5$

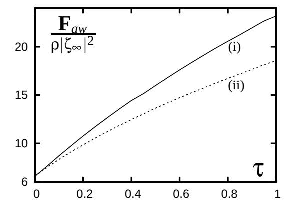

Figure 5: Added resistance for (i) a circular cylinder and (ii) a sphere

One may conclude that a proper description of the velocity field near the stagnation point influences the wave pattern near the bow greatly and that the added resistance increases significantly for increasing values of the velocity.

Numerical formulation

We now continue with the numerical formulation as proposed by Prins [21], Sierevogel [16] and applied by Bunnik [2] for the finite speed case. We write

$$
\phi_u(\mathbf{x},t) = \phi_{\mathrm{inc}}(\mathbf{x},t)+\phi(\mathbf{x},t)
$$

and we write the total unsteady perturbed potential function as a source distribution over the boundaries of the computational domain an integral expression for the velocity. The same can be done for the velocities. If $\mathbf{x}$ is inside the fluid domain, on the hull, or on the free surface, this results in

$$
\phi(\mathbf{x},t) = \iint_{\partial\Omega\backslash B}\sigma(\boldsymbol{\xi},t)\,G(\mathbf{x},\boldsymbol{\xi})\;\mathrm{d}S_\xi \qquad (44)
$$

$$
\nabla\phi(\mathbf{x},t) = (1-T)\sigma(\mathbf{x},t)\,\mathbf{n}+\iint_{\partial\Omega\backslash B}\sigma(\boldsymbol{\xi},t)\,\nabla_{\mathbf{x}}G(\mathbf{x},\boldsymbol{\xi})\;\mathrm{d}S_\xi \qquad (45)
$$

We use the following time independent source function

$$
G(\mathbf{x},\boldsymbol{\xi}) = -\frac{1}{4\pi r}-\frac{1}{4\pi r'} \qquad r = |\mathbf{x}-\boldsymbol{\xi}| \quad r' = \left|\mathbf{x}-\boldsymbol{\xi}\,'\right|
$$

where $\boldsymbol{\xi}\,'$ is the mirror of the source point with respect to the bottom and

$$
T = \begin{cases} 1 & \text{if } \mathbf{x}\in\Omega\backslash\partial\Omega \text{ or } \mathbf{x}\in B \\ \frac{1}{2} & \text{if } \mathbf{x}\in\partial\Omega\backslash B \\ 0 & \text{if } \mathbf{x}\notin\Omega \end{cases}
$$

So when the source strength is known, the velocities can be computed directly. Compared with the standard frequency-domain approaches a disadvantage of this approach is that $3N_{fs}N_h$ extra influence coefficients have to be calculated, where N_{fs} is the number of panels on the free surface and N_h the number of panels on the hull. Furthermore, these coefficients have to be stored in the computer's memory, because the pressure on the hull must be evaluated at each time step. In principle expressions (44,45) can be substitited in the no flux condition on the hull and the linearised free-surface condition (20). In the classical frequency domain approach with free-surface condition (21) the Neuman condition at the hull gives rise to a Fredholm integral equation of the second kind, if one chooses a source function that fulfills condition (20) as well.

Here the situation is more complicated because of the time derivatives and spatial derivatives of the potential at the free surface. We use a uniform time step, Δt. For the time derivatives we introduce second order difference schemes

$$\frac{\partial^2 \phi}{\partial t^2}^i = \frac{1}{(\Delta t)^2}\left(2\phi^i - 5\phi^{i-1} + 4\phi^{i-2} - \phi^{i-3}\right) + O\left((\Delta t)^2\right) \quad (46)$$

$$\frac{\partial \phi}{\partial t}^i = \frac{1}{\Delta t}\left(\frac{3}{2}\phi^i - 2\phi^{i-1} + \frac{1}{2}\phi^{i-2}\right) + O\left((\Delta t)^2\right) \quad (47)$$

The discretization of the unsteady potential's space derivatives is more difficult. To see how to proceed, we rewrite the free-surface condition (20), where we also use the difference schemes for the time derivatives, (46) and (47).

$$\begin{aligned}
&\phi^i\left(\frac{2}{(\Delta t)^2} - \frac{T}{gS}\frac{3}{2\Delta t}\right) + \nabla\Phi_s\cdot\nabla\left(\nabla\Phi_s\cdot\nabla\phi^i\right) + \\
&\left(2\frac{3}{2\Delta t} - \frac{T}{gS}\right)\nabla\phi^i\cdot\nabla\Phi_s + g\frac{\partial\phi^i}{\partial z} + \qquad (48)\\
&\frac{1}{2}\left(\frac{\partial\phi}{\partial x}^i\frac{\partial}{\partial x_{\zeta_s}} + \frac{\partial\phi}{\partial y}^i\frac{\partial}{\partial y_{\zeta_s}}\right)\|\nabla\Phi_s\|^2 = f \quad \text{on } z = \zeta_s
\end{aligned}$$

where T is the transfer term

$$T = \frac{\partial}{\partial z}\left(\frac{1}{2}\left(\frac{\partial\Phi_s}{\partial x}\frac{\partial}{\partial x_\zeta} + \frac{\partial\Phi_s}{\partial y}\frac{\partial}{\partial y_\zeta}\right)\|\nabla\Phi_s\|^2 + g\frac{\partial\Phi_s}{\partial z}\right) \quad \text{on } z = \zeta_s \qquad (49)$$

and S is an abbreviation for

$$S = 1 + \frac{1}{2g}\frac{\partial}{\partial z}\|\nabla\Phi_s\|^2 \quad (50)$$

f is a function that depends on the history of the potential

$$f = \frac{5\phi^{i-1} - 4\phi^{i-2} + \phi^{i-3}}{(\Delta t)^2} + \left(2\nabla\Phi_s\cdot\nabla - \frac{T}{gS}\right)\frac{\left(2\phi^{i-1} - \frac{1}{2}\phi^{i-2}\right)}{\Delta t}$$

We will discuss in detail only the derivative of ϕ in the direction of the steady velocity, $\nabla\Phi_s$, the other terms need similar considerations. Because the steady velocity is parallel to the steady free surface, this is a tangential derivative. Although the collocation points lie on the curved, steady free surface, $z = \zeta_s$, this derivative can be obtained by numerical differentiation in the flat x,y-plane. To make this clear, we make use of the partial derivative $\frac{\partial}{\partial x_{\zeta_s}}$ and $\frac{\partial}{\partial y_{\zeta_s}}$, and rewrite the derivative into

$$\begin{aligned}
\nabla\Phi_s\cdot\nabla\phi &= \frac{\partial\Phi_s}{\partial x}\frac{\partial\phi}{\partial x} + \frac{\partial\Phi_s}{\partial y}\frac{\partial\phi}{\partial y} + \left(\frac{\partial\zeta_s}{\partial x}\frac{\partial\Phi_s}{\partial x} + \frac{\partial\zeta_s}{\partial y}\frac{\partial\Phi_s}{\partial y}\right)\frac{\partial\phi}{\partial z}\\
&= \frac{\partial\Phi_s}{\partial x}\frac{\partial\phi}{\partial x_{\zeta_s}} + \frac{\partial\Phi_s}{\partial y}\frac{\partial\phi}{\partial y_{\zeta_s}}
\end{aligned}$$

where we used the steady kinematic free-surface condition in the first step. So, if we consider the potential on the free surface to be a function of x and y only, the tangential derivative can be obtained by means of very simple difference schemes for a flat plane. To determine $\nabla\Phi_s\cdot\nabla\phi$, we use a second-order upwind difference scheme. In this difference scheme, only collocation points are used that are upstream of the collocation point where the derivative is required, and of course that collocation point itself. This ensures a numerically-stable time integration. It can be shown that central difference schemes mostly lead to instable schemes, whereas upwind schemes never do.

The difficulty in obtaining this derivative is that the collocation points are mostly not in the direction of the steady flow, because our grid only approximately follows the steady stream lines, as shown in figure 6. For simplicity, we assume here that the panels are rectangular, and all have the same size. To obtain two values of the potential in the direction of the steady flow, we interpolate the potential from two nearby collocation points with the same x-coordinate, which results in the values of the potential with second-order accuracy on the positions marked with an '$\circ$' in figure 6. Higher-order interpolation does not lead to higher-order accuracy, because the accuracy of the potential is only of second order in a first-order panel method. In the difference scheme we now use the potential in the point $\mathbf{x}$ itself, and in the points where we interpolated the potential, $\mathbf{x}_1 = \mathbf{x} - \Delta s\frac{\nabla\Phi_s}{\|\nabla\Phi_s\|}$ and $\mathbf{x}_2 = \mathbf{x} - 2\Delta s\frac{\nabla\Phi_s}{\|\nabla\Phi_s\|}$, which results in

$$\nabla\Phi_s\cdot\nabla\phi = \|\nabla\Phi_s\|\frac{\frac{3}{2}\phi(\mathbf{x}) - 2\phi(\mathbf{x}_1) + \frac{1}{2}\phi(\mathbf{x}_2)}{\Delta s} + O\left((\Delta s)^2\right) \quad (51)$$

This is a second-order scheme if the potentials are free of errors. Unfortunately, the potentials contain errors due to the discretization of the source distribution, the discretization of the boundaries, and the interpolation. This error is of second order in the panel size, which means that the derivative (because of dividing by Δs) contains a first-order error. Because in each interpolation two collocation points are

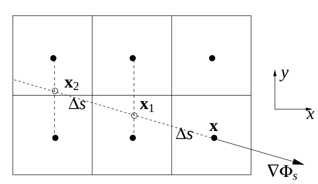

Figure 6: Example of the method to determine the difference scheme for $\nabla\Phi_s\cdot\nabla\phi$.

used, the final difference scheme includes maximal 5 of the N_{fs} free-surface collocation points, so it looks like

$$\nabla\Phi_s\cdot\nabla\phi(\mathbf{x}_i) = \sum_{j=1}^{N_{fs}}\alpha_{ij}\phi(\mathbf{x}_j) \quad (52)$$

If i is kept constant, at most 5 of the α_{ij} are non-zero. If panels of non-rectangular shape are used, equation (51) slightly changes, but the idea remains the same. Because our computational free surface is limited in size, this method cannot be applied on the last row of panels on its upstream edge. Because there are no upstream panels, it is not possible to use an upwind difference scheme. If $\tau = \omega U/g > \frac{1}{4}$, this can easily besolved by imposing the condition $\phi = 0$ on these panels, because wavescannot propagate in the upstream direction. Therefore, apart from incoming waves, no waves exist. If $\tau < \frac{1}{4}$, waves can also propagate in upstream direction. In that case, the condition $\phi = 0$ can also be imposed, as long as a damping zone, that damps the waves sufficiently, is placed between the ship and the upstream edge of the computational domain. In that case, the waves have vanished by the time they have reached the last row of panels, and the condition $\phi = 0$ makes sense. This means that, if $\tau < \frac{1}{4}$, the size of the computational domain in front of the ship may have to be be quite large because the appropriate damping zone has to fit. If the speed of the ship is sufficiently small, central or downwind difference schemes can also be used. No special condition has to be imposed on the last row of panels in that case.

Accuracy and stability analysis

We will discuss one aspect of the scheme in detail. We compare thecontinuous dispersion relation with the dispersion relation of the discretised scheme. This analysis can be carried out analytically for the case of deep water and the simpified free surface condition (21). The double Fourier transform of the source function at the raised panel surface $z = z_{fs}$ becomes

$$\tilde{G}(\alpha,\beta) = -\frac{e^{i\alpha x + i\beta y - z_{fs}\sqrt{\alpha^2+\beta^2}}}{2\sqrt{\alpha^2+\beta^2}}. \tag{53}$$

The Fourier transform of the $z-$derivative of the source function becomes

$$\tilde{Q}(\alpha,\beta) = \sqrt{\alpha^2+\beta^2}\,\tilde{G}(\alpha,\beta). \tag{54}$$

The Fourier transform for the source strenght at the free surafce then becomes, with $\alpha = k\cos\theta$ and $\beta = k\sin\theta$,

$$\widetilde{W}\tilde{\sigma} := \tilde{G}(-\omega^2 + 2Uk\omega\cos\theta - U^2k^2\cos^2\theta + gk)\tilde{\sigma} = \widetilde{RHS}. \tag{55}$$

Application of the inverse transform leads to wave contributions at the zeros of the continuous dispersion relation

$$-\omega^2 + 2Uk\omega\cos\theta - U^2k^2\cos^2\theta + gk = 0. \tag{56}$$

The two solutions of the dispersion relation are

$$k_{\pm} = \begin{cases} \frac{g}{4U^2\cos^2\theta}\left(1 \pm \sqrt{1+4\tau\cos\theta}\right)^2 & \text{if } 1+4\tau\cos\theta \geq 0, \\ \frac{g}{4U^2\cos^2\theta}\left(1 \pm i\sqrt{-1-4\tau\cos\theta}\right)^2 & \text{if } 1+4\tau\cos\theta < 0. \end{cases} \tag{57}$$

We will study only source-discretization effects, so we assume that the time and space derivatives of ϕ in the Kelvin condition are obtained exactly, without any error, which leaves us with the following discrete dispersion relation

$$-\omega^2 + 2Uk\omega\cos\theta - U^2k^2\cos\theta^2 + g\frac{\widehat{G}}{\widehat{Q}} = 0,$$

where $\widehat{G}$ is the discrete Fourier transform of $G_{i,j}$, defined as

$$G_{m-i,n-j} = \int_{(i-\frac{1}{2})\Delta x}^{(i+\frac{1}{2})\Delta x}\int_{(j-\frac{1}{2})\Delta y}^{(j+\frac{1}{2})\Delta y} \frac{-\,d\xi\,d\eta}{4\pi\sqrt{(x_m-\xi)^2+(y-\eta)^2+z_{fs}^2}}$$

and $\widehat{Q}$ is the discrete Fourier transform of the derivative with respect to z of $G_{i,j}$. In our analysis we will only consider the roots, in (57), with the '-' sign and omit the root with the '+' sign because the latter usually corresponds to a short wave which cannot berepresented accurately on the free-surface grids that we use and will damp very fast. The only discretizations left are the panel size and the distance from the raised-panel surface to the free surface, z_{fs}. It turns out that if the collocation points are chosen below the centre of a panel like we chose them, the numerical damping is zero. Numerical damping is very useful to suppress instabilities, so we will introduce damping by choosing appropriate difference schemes. Damping can also be introduced by shifting the collocation points upstream like Raven [1] did, but that is not done here. Because the damping is zero, we will only study the effect of the source discretization on the dispersion.

Figure 7 shows what happens to the dispersion of several downstream waves when we increase the distance $z_{fs} = \mu\sqrt{\Delta x \Delta y}$ from the free surface to the raised- panel surface for several values of τ and a fixed Froude number $Fn = 0.4$. The reference length L in this Froude number is taken to be one in all the calculations in this chapter. We introduce the non-dimensional longitudinal and transverse wave numbers $\widehat{\alpha}$ and $\widehat{\beta}$

$$\widehat{\alpha} = \frac{k\Delta x\cos\theta}{2\pi} \qquad \widehat{\beta} = \frac{k\Delta y\sin\theta}{2\pi}$$

$\widehat{\alpha} = 0.05$ means we use 20 panels per longitudinal wavelength. κ is the ratio of transverse panel size Δy and longitudinal panel size Δx. It seems that, when μ increases, the dispersion becomes less in all cases and eventually approaches zero. This was also observed by Raven [1] for the steady case. We may conclude that it is sufficient to use $\mu = 1$ in the calculations, because far all τ and angles, the dispersion is very small compared with the $\mu = 0$ case. Figure 8 shows what happens to the dispersion of a wave with

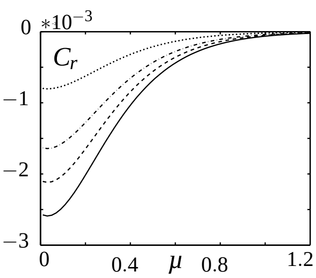

Figure 7: Dispersion for $\tau = 5,\ 1,\ 0.5,\ 0.25$ (top down), $Fn = 0.4$, $\theta = 0$, $\kappa = 1$, $\widehat{\alpha} = 0.05$.

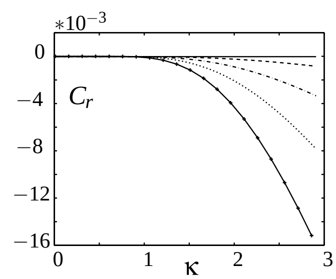

Figure 8: Dispersion for $\theta = 0,\ \pi/8,\ \pi/4,\ 3\pi/4,\ \pi/2$ (top down), $Fn = 0.4$, $\widehat{\alpha} = 0.05$, $\mu = 1$, $\lambda = 1$.

length $\lambda = 1$ at various downstream angles if we increase the ratio $\kappa = \frac{\Delta y}{\Delta x}$ and keep Δx constant. We see that for waves with zero wave angle, so for waves propagating along the x-axis, it does not matter how large the transverse panel size Δy is. When we increase the wave angle to $\frac{\pi}{2}$ with steps of $\frac{\pi}{8}$, the dispersion depends more and more on the transverse panel size, which could be expected since $\theta = \frac{\pi}{2}$ corresponds to a transverse wave. Again we see that a small transverse panel size is only important for (nearly) transverse waves. It seems that $\kappa = 1$ is a good choice; little dispersion in all cases and yet it is not too small, so the number of transverse panels will not be too large. In the work of Bunnik [2] also a similar motivation is given for the proper choice of the difference schemes.

Results for an LNG carrier

We apply our model to a 125,000 m^3 LNG carrier sailing at

Froude numbers $Fn = 0.14$, $Fn = 0.17$ and $Fn = 0.2$ in water with a depth $h = 175$ metres. The main particulars of the LNG carrier are listed in table 1. We compare our predictions for the motions of the ship and the added resistance at these Froude numbers with measurements from MARIN. Results are shown wave angles $\theta = 0$ (head waves) and $\theta = \frac{\pi}{4}$ (bow-quartering waves). We also vary the length of the incoming waves.

Figure 9 shows the hull paneling that is used in the calculations. The total carrier was divided into 2380 panels, but because we make use of symmetry relations, we only used the starboard side of the ship in the calculations, leaving 1190 panels. There were 70 panels along the waterline of the ship and 17 at each frame.

Figure 10 shows the steady wave pattern of the LNG carrier when it sails at Froude number $Fn = 0.2$. To calculate it, RAPID used 60 panels per wavelength, and 14 panels in transverse direction.

Denomination	Symbol	Unit	Value
Length	L	m	273
Breadth	B	m	42
Draught	T	m	11.5
Displacement	Δ	m^3	98740
Block coefficient	C_B	[-]	0.749
Longitudinal centre of gravity from aft perpendicular	$\overline{AG}$	m	138.66
Centre of gravity above base	$\overline{KG}$	m	13.7
Longitudinal gyradius	k_{yy}	% L	24
Transverse gyradius	k_{xx}	% B	35
Natural heave period	T_z	s	9.4
Natural pitch period	T_θ	s	9.4
Natural roll period	T_ϕ	s	16

Table 1 : Main particulars of the LNG carrier.

In the computer code we may choose the steady potential. The RAPID steady potential is used in to compute the added resistance for three values of the Froude number. To do so first the first order quantities such as the added mass(moment) and damping matrices must be computed. Taking into account first order motions the added resistance is computed and compared with experimental values obtained at MARIN. The results for head seas and bow-quartering waves are shown in Figure 11 and 12. The computed and measured results are given for $Fn = 0.2,\ 0.17,\ 0.14$ top-down. The dependency of the added resistance on forward speed, Figure 11, shows a similar character as the the asymptotic results for small values of the wavelength, Figure 5, where the motion of the vessel is negligable. Figure 13 shows the added resistance computed

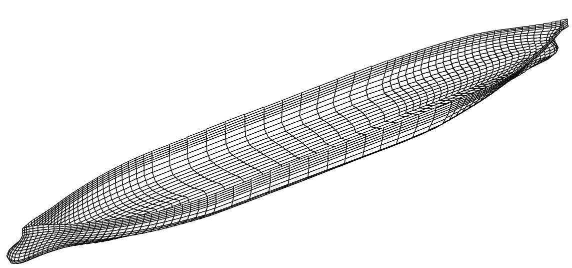

Figure 9: Hull paneling of LNG carrier for Froude number 0.2.

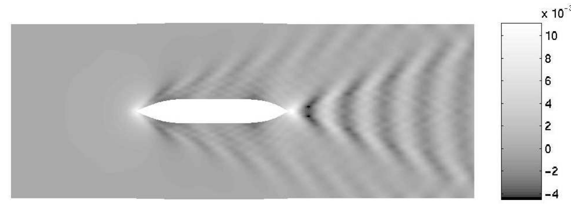

Figure 10: Steady wave pattern, scaled with the length of the ship, $Fn = 0.2$.

with the non-linear flow (top), the double-body flow (middle) and the uniform flow (bottom). Although the predicted motions of the ship were not that much different, we see large differences between the predicted added resistances. The use of the double-body flow, for these Froude numbers, results in a large underestimation of the added resistance, and the use of the uniform flow in a huge underestimation of the added resistance. These underestimations cannot be caused by the small differences between the predicted motions. Therefore, there must be another explanation. Since the differences between the predicted added resistances do not seem to be caused by the first-order fluid quantities on the hull of the ship (otherwise there would have been larger differences between the motions), nor the motions, they must be caused by the predicted wave elevation on the steady waterline of the ship. In Figure 14 we show the added

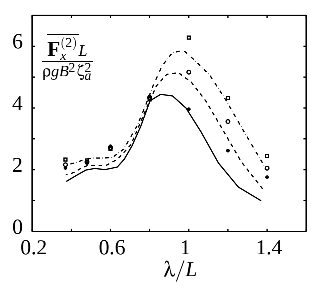

Figure 11: Added resistance in head waves

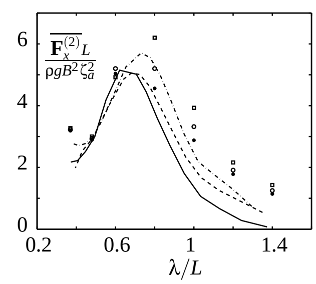

Figure 12: Added resistance in bow-quartering waves

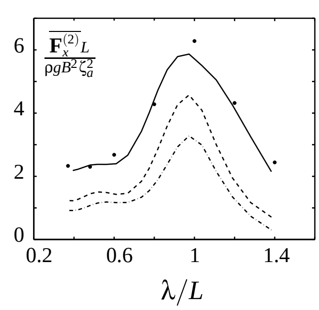

Figure 13: Added resistance in head waves and for $Fn = 0.2$. The asterisks correspond to measurements.

resistance [23] for a cruise vessel, with transom stern, sailing at a speed of 20 knots in head waves. The computations are carried at MARIN by means of three different methods. The results obtained by means of the time-domain code FATIMA based on [2] shows an improvement especially for short waves. These results compare well with the asymptotic, slow speed, results shown in Figure 5. The influence of the local steady flow field and wave height on the wave interaction near the bow turns out to be essential for the computation of the added resistance, both for high speed and low speed vessels.

Acknowledgement

The author is grateful to Hoyte Raven and Tim Bunnik of MARIN for their suggestions and for the material they made available.

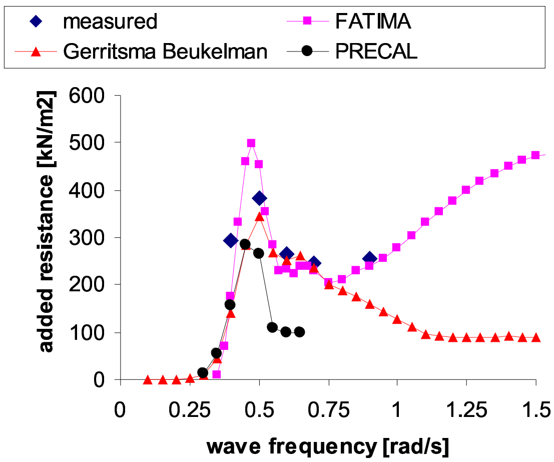

Figure 14: Comparison of methods to compute added resistance

References

[1] H.C. Raven, *A solution method for the non-linear ship wave resistance problem*, PhD thesis, TUDelft, Delft (1996)

[2] T.H.J. Bunnik, *Seakeeing calculations for ships, taking into account the non-linear steady waves*, PhD thesis, TUDelft, Delft (1999).

[3] E. Baba and K. Takekuma, A study on free-surface flow around bow of slowly moving full forms, *J. Soc. of Naval Arch. Japan* **137** (1975).

[4] E. Baba and M. Hara, Numerical evaluation of a wave-resistance theory for slow ships, *Proc. of the 2nd Int. Conf. on Numerical Ship Hydrodynamics*, Berkeley (1977) 17-29.

[5] J.N. Newman, Linearized wave resistance theory, *Proceedings of the Int. seminar on wave resistance*, Soc. of Naval Arch. Japan (1976).

[6] K. Eggers, Non-Kelvin dispersive waves around non-slender ships, *Schiffstechnik*, **28** (1981).

[7] F.J. Brandsma, *Low Froude number expansions for the wave pattern and the wave resistance of general ship forms*, PhD thesis, TUDelft, Delft, (1987).

[8] T.F. Ogilvie, *Wave resistance: the low-speed limit*, report no. 002,Univ. of Michigan, Dept of Nav. Arch. Mar. Eng., Ann Arbor (1967).

[9] F.J. Brandsma and A.J. Hermans, A quasi linear free surface condition in slow ship theory, *Schiffstechnik*, **32** (1985) 25-41.

[10] C.W. Dawson, A practical computer method for solving ship-wave problems, *Proc. of the 2nd Int. Conf. on Numerical Ship Hydrodynamics*, Berkeley (1977) 30-38.

[11] P.D. Sclavounos and D.E. Nakos, Stability analysis of panel methods for free-surface flows with forward speed, *Proc. of the 17th Symp. on Naval Hydrodynamics*, Den Haag (1988) 173-194.

[12] H. Raven, Inviscid calculations of ship wave making, capabilities, limitations and prospects, *Proc. of the 22nd Symp. on Naval Hydrodynamics*, Washington DC (1998) 738-754.

[13] J.N. Newman, The theory of ship motions, *Advances in Applied Mechanics*, **18** (1978).

[14] V. Bertram, *A 3-d Rankine panel method to compute added resistance of ships*, Technical report 566, TU of Hamburg (1996).

[15] R. Timman and J.N. Newman, The coupled damping coefficients of a symmetric ship, *J. of Ship Research*, **5** (1962) 1-7.

[16] L.M. Sierevogel, *Time-domain calculations of ship motions*, PhD thesis, TUDelft, Delft (1998).

[17] D. Givoli, *Numerical methods for problems in infinite domains*, Elsevier, Amsterdam (1992).

[18] A.J. Hermans, Slowly moving hull forms in short waves, *J. of Engineering Mathematics*, **25** (1991), 63-75.

[19] S. Kalske, Added resistance and unsteady bow wave field of a ship in short waves, *Acta Politechnica Scandinavia, mechanical engineering series* **133**, Finnish Ac. of Techn., Espoo (1998), 96 pp.

[20] T. Sakamoto and E. Baba, Minimization of resistance of slowly moving hull forms in short waves, *Proc. 16th Symposium on Naval Hydrodynamics*, Berkeley (1986) 598-612.

[21] H.J. Prins, *Time-domain calculations of drift forces and moments*, PhD thesis, TUDelft (1995).

[22] A.J. Hermans, The diffraction of short free-surface water waves, a uniformexpansion, *Wave Motion*, **18** (1993) p 103-119.

[23] T.H.J. Bunnik, Validation of a prediction method for the added resistance of ships, *Proc. of the 8th Int. Conf. on Numerical Ship Hydrodynamics*, Busan, Korea (2003).